Determining the site preference of trivalent dopants in bixbyite sesquioxides by atomic-scale simulations

C. R. Stanek,* K. J. McClellan, B. P. Uberuaga, and K. E. Sickafus

Los Alamos National Laboratory, MST-8 Structure and Property Relations, Los Alamos, New Mexico 87545, USA

M. R. Levy and R. W. Grimes

Department of Materials, Imperial College London, London SW7 2BP, United Kingdom

Oxides with the bixbyite structure ($Ia\bar{3}$) have two crystallographically unique cation sites, namely (in Wyckoff notation) $24d$ and $8b$. Since the symmetries of these two sites are different (C_2 and S_6, respectively), properties related to solute cations will vary depending on the site preference. Therefore, we have employed atomic scale simulation techniques to systematically investigate the solution site preference of a range of trivalent cations ranging from Sc^{3+} to La^{3+} in A_2O_3 bixbyite oxides (where A ranges from Sc to La). Results reveal that when the solute cation is smaller than the host lattice cation, the $24d$ site is energetically favorable, but when the solute cation is larger than the host lattice cation, the $8b$ site is preferred. We also discuss the tendency for solute cations to cluster, as well as corroboration of this work by first principles methods.

I. INTRODUCTION

Binary sesquioxides with the cubic bixbyite structure have broad technological significance, from radiation tolerance[1] to diluted magnetic semiconduction.[2] Although the luminescent properties of rare earth doped Y_2O_3 have been exploited for some time,[3] it is only recently that rare earth doped Lu_2O_3 has been investigated as a potential scintillator.[4] Although the crystal structure of bixbyite (Mn_2O_3, $Ia\bar{3}$) was essentially solved by Pauling and Shappell[5] over 70 years ago, the complexities of the structure have motivated still further studies.[6,7]

Bixbyite can be thought of as an oxygen deficient fluorite (e.g., CeO_{2-x}), where the lattice parameter is doubled and a quarter of the oxygen atoms are removed. Unlike fluorite, there are two unique cation positions due to the ordered arrangement of the oxygen atoms. There are 3 times as many of the so-called $24d$ sites as $8b$ sites. These sites are conveniently described by considering the cation surrounded by anions occupying six corners of a (fluorite lattice) cube, as illustrated in Fig. 1. For the $24d$ site, the unoccupied positions are on opposite corners of one cube face, while for the $8b$ site, the unoccupied positions are diagonally opposed. Furthermore, the $24d$ coordination cube is distorted, with three distinct metal-oxygen distance pairs (conversely for the $8b$ site, the six metal-oxygen distances are equal). The $24d$ distortion originates when the oxygen atoms beneath the unoccupied positions (labeled 1 and 2 in Fig. 1) are displaced toward the vacant sites, thereby increasing the O^1-A-O^2 angle so that it is the largest angle in the coordination cube. O atoms labeled 3 and 4 are farthest from the A atom, while O atoms in the same plane as the unoccupied positions (labeled 5 and 6 in Fig. 1) are nearest to the A atom and have the smallest O-A-O angle.[7] However, the mean of the three pairs of $24d$ A-O distance is practically the same as the $8b$ A-O distance.[6]

Figure 1 also shows how the symmetries of the two lattice cation sites differ. The $24d$ site is noncentrosymmetric (C_2

symmetry), while the $8b$ site is centrosymmetric (S_6 or C_{3i} symmetry). Due to these different symmetries, $24d$ cations are expected to have spectroscopic properties that are distinct from $8b$ cations. In the specific case of scintillators, the parity selection rule forbids electronic-dipole transitions between levels of the same parity, such as transitions within the f shell. However, this rule can be relaxed when a rare earth ion occupies a site without inversion symmetry, which leads to uneven crystal field components.[8] For example, in the specific case of $Eu:Lu_2O_3$, it has been proposed that it is desirable to have Eu^{3+} activator cations residing solely on $24d$ sites.[9] In this case, f-f electric dipole transitions are forbidden for Eu^{3+} cations in centrosymmetric positions (e.g., S_6 symmetry, $8b$ site), and only magnetic dipole transitions are possible.[10,11] However, since the parity selection rule is relaxed for noncentrosymmetric positions (e.g., C_2 symmetry, $24d$ site), both magnetic and electric dipole transitions are possible. As there are fewer possible transitions from the $8b$ site, slower emission and increased probability of nonradiative transitions are expected.[9]

The previous example illustrates the importance of site specific solution in bixbyite oxides, yet one of the remaining uncertainties regarding these compounds is the site preference and distribution of solute cations. In this paper, we present atomistic simulation results regarding the solution site preference of a wide range of solute cations (Sc^{3+} and In^{3+}, Lu^{3+} to La^{3+}) in A_2O_3 bixbyite oxides (where A ranges from Sc-La; Pr_2O_3-La_2O_3 are not stable in the cubic structure, but are included for the establishment of compositional trends). The aim of this study is to improve the fundamental understanding of site specific solution behavior. With this insight, we anticipate the development of optimized bixbyite oxides for scintillator and other applications requiring site specific solution. However, from a computational point of view, there is nothing remarkable about bixbyite oxides. Rather, the general method of establishing compositional trends (in this case identifying the site preference of solution cations) through the consideration of a wide range of com-

134101-1
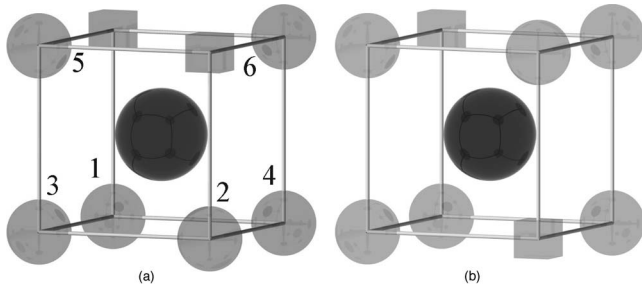
FIG. 1. The two cation sites of cubic A_2O_3 bixbyite, where the dark spheres represent A cations, the light spheres denote O and the cubes are unoccupied oxygen positions. (a) $24d$ (C_2 symmetry). (b) $8b$ (S_6 symmetry).

pounds is readily transferable to other material systems. Additionally, this approach is most effective when used in conjunction with experiment to compliment and guide further investigation.

Previous work. The solution site preference of rare earth cations in bixbyite sesquioxides has been the subject of debate for some time (Table I provides a summary). A majority of previous studies have considered rare earth solution in Y_2O_3. For example, Mandel used electron paramagetic resonance (EPR) to determine that Yb^{3+} replaces Y^{3+} on both sites in Y_2O_3.[12] Mitric *et al.* also investigated the solution of Yb^{3+} in Y_2O_3 via a combination of x-ray diffraction and magnetic susceptibility studies but found a weak $24d$ preferential occupation.[13] At low Yb^{3+} concentrations, (specifically in $Yb_{0.06}Y_{1.94}O_3$), Mitric *et al.* found the $24d$ site to be occupied exclusively.[13] Rodic *et al.* employed similar techniques to determine the site occupancy of Gd^{3+}, Dy^{3+}, Ho^{3+}, and Er^{3+} in Y_2O_3.[14] From these studies, they found that Gd^{3+} preferentially resides on the $24d$ site, while Dy^{3+}, Ho^{3+}, and Er^{3+} are randomly distributed. In a separate study, Mitric *et al.* further found with similar methods that Gd^{3+} exclusively resides on the $24d$ site in concentrations less than $x = 0.41$ (in $Gd_xY_{2-x}O_3$).[15] Hintzen and van Noort concluded from ^{151}Eu Mössbauer spectroscopy results that Eu^{3+} is randomly distributed over both $24d$ and $8b$ sites in Sc_2O_3, In_2O_3, Lu_2O_3, Y_2O_3, and Gd_2O_3.[16] However, in that study, the Mössbauer spectra could only be decomposed into two separate Lorenztian lines (corresponding to the $24d$ and $8b$ lattice sites) for $Eu:In_2O_3$ and $Eu:Sc_2O_3$.

Eu^{3+} doping in Y_2O_3 and Lu_2O_3 has received particular attention, due to both the technological significance of these compositions and also the inconsistency of the results. For example, Grill and Schieber concluded from magnetic susceptibility results that Eu^{3+} ions prefer $24d$ sites in Y_2O_3 and Lu_2O_3.[17] However, after a recommendation from van Vleck, Kern and Kostelecky repeated these measurements and found a different result at low Eu concentrations, suggesting a random distribution of Eu^{3+} ions in Y_2O_3.[18] A similar result was found by Antic *et al.*, again using magnetic susceptibility data as well as x-ray diffraction.[19] Concas *et al.* similarly concluded a random distribution of Eu^{3+} ions in both bulk and nanocrystalline Y_2O_3, using Mössbauer spectroscopy.[20] Concas *et al.* also concluded that Eu^{3+} was randomly distributed in nanocrystalline Lu_2O_3.[20] A later study confirmed this observation, but also found a $24d$ preference ($\approx 85\%$ of Eu^{3+}

TABLE I. Summary of previous site preference results.

Host lattice	Activator	Site preference	Reference
Y_2O_3	Yb	Random	12
Y_2O_3	Yb	Weak $24d$	13
Y_2O_3	Gd	$24d$	14
Y_2O_3	Gd	$24d$	15
Y_2O_3	Dy, Ho, Er	Random	14
Sc_2O_3-Gd_2O_3	Eu	Random	16
Y_2O_3, Lu_2O_3	Eu	$24d$	17
Y_2O_3	Eu	Random	18
Y_2O_3	Eu	Random	19
Y_2O_3	Eu	Random	20
Lu_2O_3	Eu	$24d$	21
Lu_2O_3	Eu	$8b$	9

on $24d$ sites) in bulk ceramic Lu_2O_3.[21] Finally, Zych investigated the energy transfer between Eu^{3+} ions occupying both sites in Lu_2O_3, as a function of Eu^{3+} concentration.[9,11] At low concentrations (e.g., 0.2 mol %), Zych found the emission spectra to be dominated by $8b$ luminescence. At higher concentrations, the $24d$ luminescence intensity was found to increase at the expense of the $8b$, although $8b$ luminescence was never completely diminished up to an Eu concentration of 10%. That the $24d$ luminescence occurs at the expense of $8b$ suggests rather efficient $8b$-$24d$ energy transfer, and the remaining $8b$ luminescence at high Eu concentrations suggests either $24d$-$8b$ back transfer or isolated $8b$ cations. Nevertheless, Zych concluded that it is impossible to completely remove slow $8b$ magnetic dipole luminescence from $Eu:Lu_2O_3$.[9]

Although this paper only addresses the solution site preference in bulk materials, it is worth noting that the site solution preference for Eu^{3+} in nanocrystalline Lu_2O_3 is different than that observed from bulk ceramic Lu_2O_3.[22,23] It has been proposed that this difference originates from the nanophase material trapping in a nonequilibrium structure.[22]

II. METHODOLOGY

Atomistic simulation calculations were carried out using a Born-type, ionic description of the lattice[24] and the Buckingham potential[25] to describe the short range interactions between ions, so that the lattice energy can be expressed as

$$E = \frac{1}{2}\sum_i \sum_{j \neq i} \left[\frac{q_i q_j}{4\pi\epsilon_0 r_{ij}} + A_{ij} \exp\left(-\frac{r_{ij}}{\rho_{ij}}\right) - \frac{C_{ij}}{r_{ij}^6} \right], \quad (1)$$

where q_i and q_j are the charges of the ions i and j, ϵ_0 is the permittivity of free space, r_{ij} is the interionic separation, and A_{ij}, ρ_{ij}, and C_{ij} are the adjustable potential parameters specific to each ion pair. All parameters were previously derived: O^{2-}-O^{2-} by Vyas *et al.*[26] and the remainder by Levy *et al.*[27] (though all were derived in the same self-consistent manner). These potentials have been used to successfully model defect behavior in other rare earth oxide systems such
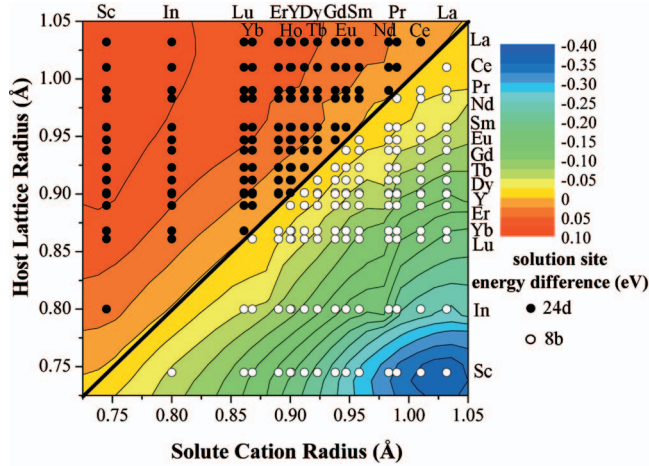
FIG. 2. (Color) Contour plot describing the energy difference between solute cations on 24d and 8b sites in A_2O_3 bixbyites, where the host lattice cation is on the ordinate and the solute cation is on the abscissa. Each point refers to a specific combination of host lattice and solute cation for which a calculation was performed.

FIG. 3. The energy difference between solute cations residing on 24d (C_2 symmetry) and 8b (S_6 symmetry) sites as a function of the ratio of solute and host lattice cationic radius.

as perovskites[28,29] and garnets.[30] The electronic polarizability of oxygen is accounted for by the shell model of Dick and Overhauser,[31] where a massless shell of charge $-2.04|e|$ is coupled to a massive core of charge $0.04|e|$ by an isotropic, harmonic force constant, k (6.3 eV/Å^2).

The above techniques can be used to describe forces between ions in perfect lattice structures or in a defective lattice. Defect energies are calculated by partitioning the lattice into a region I (≈ 10 Å) and region II (extending to infinity). A defect is incorporated near the center of region I, and the response of the ions in region I to the defect is calculated explicitly, while the response of ions in region II is evaluated via the Mott-Littleton approximation.[32] Further information on these methods can be found elsewhere.[33]

III. RESULTS AND DISCUSSION

A. Isolated defects

The aforementioned simulation methods are especially useful in the determination of trends from relative energies across a broad compositional space. Here, the simulation results predicting the site preference of solute cations ranging in size from Sc^{3+} to La^{3+} in a series of bixbyite oxides (Sc_2O_3-La_2O_3) are presented in the form of a contour map. An advantage of this approach is that a large set of data can be presented in a manner that readily allows for the identification of compositional regions of interest. For example, Fig. 2 describes the energy difference between a solute cation residing on the 8b and the 24d site (so that negative values, represented by empty circles, correspond to an 8b preference and positive values, solid circles, correspond to a 24d preference). It is clear from Fig. 2 that for all combinations of solute cation and bixbyite host lattice, where the solute cation is different than the host lattice cation, there is a site
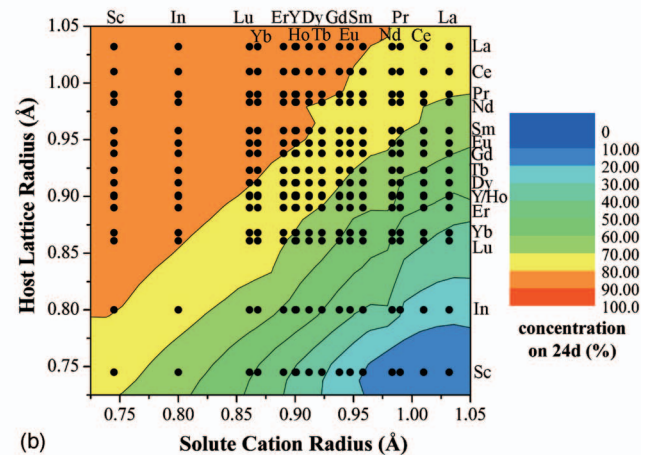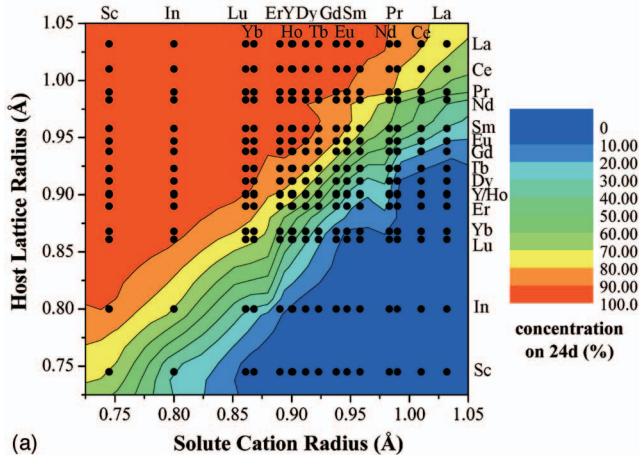
FIG. 4. (Color) Contour plots describing the concentration of solute cations residing on 24d sites as predicted by the energies from Fig. 2 via the Boltzmann distribution of Eq. (2) at two different temperatures, where a 24d concentration of 75% is random. (a) 24d concentration at 273 K. (b) 24d concentration at 1273 K.

preference for the solute cation. These preferences are unsurprisingly small when the cation radii of the solute cation and host lattice cation are similar.[34] However, as the cationic radius difference increases, the solution site preference becomes more pronounced. In particular, for all cases where the solute cation is smaller than the host lattice cation, the 24*d* site is preferred and when the solute cation is larger than the host lattice cation the 8*b* site is preferred. This prediction simply suggests that for scintillator compounds whose emission is dominated by *f* shell transitions, optimal compositions have smaller activator cations than host lattice cations (filled circles in Fig. 2). The reason for this preference is essentially crystallographic. Recall that the six metal-oxygen distances in the 8*b* site are equivalent, and that there are three unique pairs of metal-oxygen distance for the 24*d* site. Two of the metal-oxygen distances in the 24*d* site are less than the analagous distance in 8*b*. In the case of rare earth solute cations smaller than the host lattice cation, they are readily accomodated in a site with shorter bonds. However, for solute cations larger than the host lattice cation, solution at the 24*d* site leads to increased strain and an increase in solution energy.

Figure 3 shows the site preference of solute cations as a function the ratio between solute and host lattice cations. Interestingly, all the data from Fig. 2 collapses onto a single smooth curve when plotted as a function of the radius ratio and can be fit to a simple polynomial function. However, the limiting trends for radius ratios greater and less than 1 are much different. For example, an extrapolation of the trend for cases where the solute cation is larger than the host lattice cation (i.e., 8*b* preference), suggests a continual increase in energy for combinations of solute and host lattice cations with ratios larger than considered here (e.g., La : Mn_2O_3). A similar behavior is not observed for cases when the solute cation is smaller than the host lattice cation (i.e., 24*d* preference). In fact, the energy difference for radius ratios less than 1 saturates such that radius ratios smaller than 0.8 do not lead to a variation in the energy difference. Therefore, in the region where the radius ratio is less than 1, the energy difference is much less (and constant, ≈ 0.1 eV) than when the radius ratio is greater than 1.

In Fig. 2, no account is made for the fact that in the bixbyite structure, there are three times as many 24*d* sites as 8*b* sites. To rectify this, Figs. 4(a) and 4(b) predict the fractional occupancy of solute cations on 24*d* sites according to a Boltzmann distribution of the type (assuming constant entropy)

$$\frac{C_{24d}}{C_{8b} + C_{24d}} = 1 - \frac{e^{-\Delta E/kT}}{e^{-\Delta E/kT} + 3}, \quad (2)$$

where C_{8b} and C_{24d} are the concentrations of solute cations on 8*b* and 24*d* sites, respectively, and ΔE is the difference in solution energy for the solute cation between the 8*b* and 24*d* site. The temperatures used to generate Figs. 4(a) and 4(b) are 273 K and 1273 K, respectively. It is clear from Fig. 4, especially at the low temperature, that the small energy differences shown in Fig. 2 correspond to a marked preferential occupancy (recalling that 75% occupation on 24*d* sites is random). The overall site preference trend is less pronounced
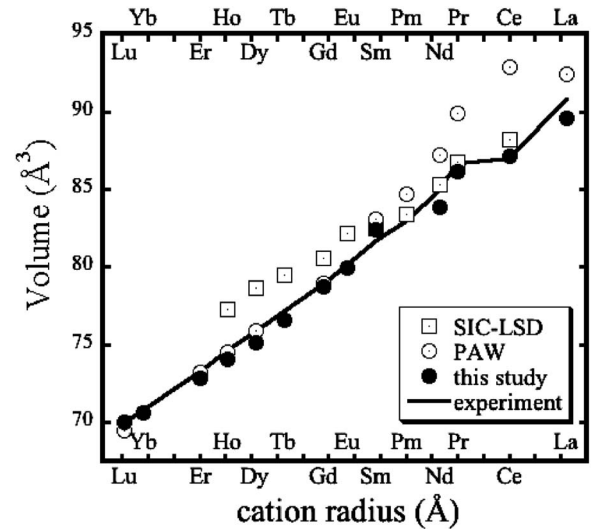
FIG. 5. A comparison of volume per molecule values for the range of cubic RE_2O_3 compounds obtained by SIC-LSD (empty squares) (Ref. 35), PAW (empty circles) (Ref. 36), pair potentials (filled circles), and experiment (line) (Ref. 37) [except for Ho_2O_3 and Dy_2O_3 (Ref. 7) and Er_2O_3 (Ref. 38)].

at the high temperature, with ΔE values corresponding to more random occupation than at low temperatures. This observation suggests that experimental data will be strongly influenced by the synthesis route of the samples examined.

B. Comparison with first principles methods

In order to verify the trends observed in Fig. 2, we have performed density functional theory (DFT) calculations. We used the VASP code[39–42] with the projector augmented-wave method[43,44] on supercells containing 80 atoms. We used both the PW91 and PBE generalized gradient approximation functionals. We tested convergence of our results versus energy cutoff, *k*-point sampling (using both gamma point and 2 × 2 × 2 *k*-point meshes of the Monkhorst-Pack type[45]), and spin polarization.

We attempted to calculate the site preference for the following configurations: Yb in Lu_2O_3, Lu in Yb_2O_3, Lu in Nd_2O_3, Nd in Lu_2O_3, Sc in Nd_2O_3, Nd in Sc_2O_3, Y in Gd_2O_3, and Gd in Y_2O_3. In most cases, we were unable to obtain convergence. This is consistent with previous DFT work on rare earth oxides.[36] In the cases where we were able to converge results, we found no significant sensitivity to the energy cutoff, *k*-point sampling, or spin polarization (to within about 0.05 eV).

Overall, we were unable to achieve quantitative agreement with our empirical potential calculations. This is due in part to the small energy differences of the site preference, but also pertains to the difficulties associated with the first principles consideration of rare earth oxides. Furthermore, there are issues with how well DFT predicts the lattice constant of the series of rare earth oxides. Previously, several first principles methods have been used to calculate the lattice volume of the cubic rare earth oxides considered here.[35,36] In fact, Fig. 5 shows that our pair potential calculations reproduce

the RE_2O_3 lattice constant across the entire rare earth series better than either the self-interaction-corrected local-spin density (SIC-LSD), which agrees well with experiment for large cations or projector augmented-wave methods (PAW), which agrees well for small cations. (Here, RE denotes a rare earth cation. Our results for Sc_2O_3, In_2O_3, and Y_2O_3 have been omitted from Fig. 5 for the sake of comparison, although these results also agree well with experimental values. We have not considered Pm_2O_3.)

Thus, as shown in Fig. 5, electronic structure methods are unable to even qualitatively capture trends in lattice constant over the entire range of rare earth oxides. The importance of this deficiency is illuminated by our finding that the energy difference between solution on $24d$ and $8b$ sites is very sensitive to lattice parameter. For the case of Sc in Nd_2O_3, if use constant volume conditions, the energy difference is about -0.1 eV ($8b$-$24d$). If we relax the volume the difference changes to 0.77 eV. Not only does the energy change by nearly 1 eV when simply changing the lattice parameter, but the predicted solution site also changes. As the DFT calculations are unable to quantitatively reproduce the lattice parameter of these oxides, and the site preference is so sensitive to lattice parameter changes, we are not confident that DFT will be successful predicting the correct site preference.

That said, the sensitivity of the site preference to variations in lattice parameter does lead to some interesting insights into these materials. First, it suggests that perhaps applied pressure can be used to influence the site preference. To the extent that dopants are kinetically trapped in the locations they occupy during synthesis, different synthesis routes might lead to different occupations. This result also suggests that the surface strain effects in nanocrystalline bixbyite oxides will likely lead to a different solution site preference than their bulk ceramic counterparts.

C. Clustered defects

It is well established that an energy transfer takes place from Eu^{3+} ions in $8b$ sites to $24d$ sites in several bixbyite compounds.[9,46–49] Furthermore, since this energy transfer takes place via a superexchange process, the probability of this type of energy transfer is a function of the distance between $8b$ and $24d$ ions.[46,50–52] Consequently, we have considered the interaction between solute cations to ascertain whether defect clusters are more favorable than isolated defects. According to the equation of Dornauf and Heber,[52]

$$P = \frac{1}{\tau_0} \exp[\gamma(R_0 - R)], \quad (3)$$

P is the probability of transfer via superexchange, which is governed by τ_0, the radiative decay time of the donor, γ, the exchange constant, R, the distance between donor and acceptor and R_0, the critical transfer radius, which is the distance at which an isolated donor-acceptor pair exhibits the same transfer rate as the radiative decay rate. Based on Eq. (3), in bixbyite oxides, the nearest neighbor $8b$-$24d$ cations are most likely to transfer energy since they are nearer to one another than any other cationic combination. However, Buijs *et al.* have determined that energy can transfer over more
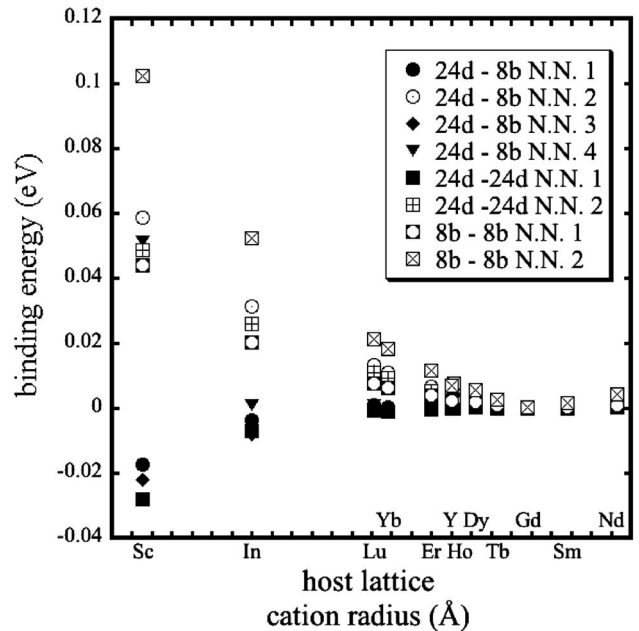
FIG. 6. Calculated binding energies for Eu-Eu solute cation clusters in different configurations in A_2O_3 oxides, where the configuration label refers to the position of the Eu cations and the nearest neighbor distance of the particular cluster.

than 7 Å (i.e., $R_0 = 7$ Å) from $8b$ to $24d$ sites in Y_2O_3 and Gd_2O_3.[46]

Figure 6 describes the predicted cluster binding energy of Eu^{3+} ions in a series of A_2O_3 compounds, where the Eu-Eu distance is less than R_0 for each configuration considered. In particular, we have calculated binding energies for the first through fourth nearest neighbor (NN) dimer clusters of $8b$-$24d$ and first and second nearest neighbor clusters of both $8b$-$8b$ and $24d$-$24d$. Table II describes representative interionic distances for these cluster configurations in Y_2O_3. We define binding energy to be the difference between the cluster energy and the sum of equivalent isolated defect energies, such that a positive value corresponds to an energetic preference for the defects to be isolated. Figure 6 shows that when the host lattice cation is similar in size to Eu^{3+} (e.g., Tb^{3+}, Gd^{3+}, and Sm^{3+}) the binding energy for all cluster configurations is practically zero. This is expected since these defects are charge neutral relative to regular lattice occupa-

TABLE II. Cluster configurations in Y_2O_3.

Configuration	Nearest neighbor	Separation
$24d$-$8b$	1	3.52 Å
$24d$-$8b$	2	3.99 Å
$24d$-$8b$	3	6.36 Å
$24d$-$8b$	4	6.64 Å
$24d$-$24d$	1	3.54 Å
$24d$-$24d$	2	4.01 Å
$8b$-$8b$	1	5.30 Å
$8b$-$8b$	2	7.50 Å

tion, and therefore should not interact electrostatically. Conversely, when the size difference of the solute and host lattice cation increases, the binding energy becomes dependent upon cluster configuration. In fact, the binding energy is surprisingly negative for certain Eu-Eu cluster configurations in both Sc_2O_3 and In_2O_3. It is important to note that for all cases, there are $8b$-$24d$ cluster configurations with a nearly zero or even negative binding energy, suggesting that there is no penalty for the inter-Eu distance to be less than R_0. For the technologically significant $Eu:Y_2O_3$ and $Eu:Lu_2O_3$, Eu^{3+} cations on $24d$ and $8b$ sites are not prevented from residing near one another, thereby allowing for the efficient transfer of energy, especially at higher concentrations of dopant.

D. Comparison to experiment

Although we are compelled to verify these predictions by comparison to experiment, there is no single systematic study regarding the solution site behavior for the compositional space we have considered. In addition, when attempting to determine an unequivocal trend from experimental studies, we are confronted with considerable variation in conclusions. We are therefore unable to categorically confirm the validity of our predictions. Nevertheless, a comparison is illuminating.

First, we predict Yb^{3+} to reside preferentially on the $24d$ site of Y_2O_3 (80.0% and 89.5% $24d$ occupation at 1273 K and 273 K, respectively). Mandel concluded from EPR results that Yb^{3+} occurs on both the $24d$ and $8b$ site[12] while Mitric *et al.* found Yb^{3+} to reside preferentially on the $24d$ site,[13] in concert with our results (see Fig. 2). We predict a very slight preference for Ho^{3+} and Er^{3+} to occupy $24d$ sites (75.3% and 76.4% for Ho and 76.7% and 82.5% for Er at 1273 and 273 K, respectively) and a similarly slight preference for Dy^{3+} to occupy $8b$ sites (74.0% and 70.1% $24d$ occupation at 1273 and 273 K, respectively). Rodic *et al.* found Dy^{3+}, Ho^{3+}, and Er^{3+} to be distributed randomly in Y_2O_3, and Gd^{3+} to prefer $24d$ sites.[14] Our results agree reasonably with Rodic *et al.*, except for Gd^{3+}, which we predict to reside preferentially on $8b$ sites. The Mössbauer spectroscopy results of Hintzen and van Noort find Eu^{3+} cations randomly distributed in Sc_2O_3, In_2O_3, Lu_2O_3, Y_2O_3, and Gd_2O_3.[16] Over that same compositional range, our predictions differ, especially for the smaller host lattice cations where we predict near exclusive $8b$ occupation. Finally, for Eu^{3+} in Lu_2O_3 and Y_2O_3, we have several experimental studies available for comparison. First, our results are at odds with those of Grill and Schieber for Eu occupation in Y_2O_3. We predict that Eu^{3+} prefers the $8b$ site (67.2% and 33.6% $24d$ occupation at 1273 K and 273 K, respectively). Grill and Schreiber concluded a $24d$ preference.[17] Kern and Kostelecky repeated the Grill and Schieber experiment and found that Eu^{3+} is randomly distributed over $24d$ and $8b$ sites, which is closer to our prediction, especially at higher temperatures. Antic *et al.*[19] and Concas *et al.*[20] also found a random distribution of Eu^{3+} in Y_2O_3.

Finally, Zych found Eu^{3+} emission luminescence in Lu_2O_3 dominated by $8b$ sites at low concentrations,[9] which is encouraging given that our calculations pertain to the dilute

limit of solute cations and predict an $8b$ preference (57.1% and 44.0% $24d$ occupation at 1273 and 273 K, respectively). Moreover, Zych observed an increase of $24d$ luminescence intensity with increasing Eu concentration. This suggests that at low concentrations, $8b$ sites are preferentially occupied, but remain isolated. At higher concentrations, more Eu^{3+} ions reside on $24d$ sites and are therefore available for energy transfer from the already occupied $8b$ sites. This observation suggests that there is no energy penalty for Eu^{3+} cations to reside at adjacent $8b$ and $24d$ sites, which is in accordance with the near zero binding energies for $24d$-$8b$ Eu clusters in Lu_2O_3 described by Fig. 6. Also, Zych decisively proposed that it is impossible to entirely remove $8b$ emission. This is likely the case for $Eu:Lu_2O_3$, but our results predict that there are certain combinations of host lattice (including solid solutions) and solute cation that would minimize $8b$ emission, e.g., $Eu:Sc_2O_3$.

That our results are not completely verified by experimental studies is not entirely discouraging. Figure 4 clearly indicates that temperature strongly influences the distribution of solute cations. Most experimental studies have been performed on material systems where the cationic radius of the solute cation is similar to host lattice cation, which is also where we predict the distribution to be nearest to random. Furthermore, it is quite possible that higher temperature solute distributions have been effectively frozen in, thereby leading to measurements of less pronounced site preference measurements than predicted here. However, our results are less effective in the prediction of quantitative values and more useful when employed to highlight regions of compositional interest based upon relative energies. In particular, the site preference predictions made here may aid in the identification of new candidate compositions or solid solutions that create a balance between various materials properties.

IV. CONCLUSION

Atomistic simulation techniques have been used to investigate the solution behavior of trivalent cations in a range of bixbyite oxides. Our results predict that when the solute cation is smaller than the host lattice cation, the solute cation prefers to reside on the $24d$ site, though when the solute cation is larger, there is a preference for the $8b$ site. As the size mismatch increases, the specific preference also increases, except when the solute cation is much smaller than the host lattice cation (e.g., $r_{solute}/r_{host} \lesssim 0.8$) and the site preference is constant. Additionally, we have considered the potential for solute cations to cluster. For Eu^{3+} solution in A_2O_3, there is always a $24d$-$8b$ cluster configuration which has a near zero or negative binding energy. Consequently, Eu^{3+} cations can be near enough to one another to allow energy transfer. Finally, we have compared our results to existing experimental studies. The aim of this work is to stimulate further studies, both theoretical and experimental, in an effort to engineer compositions that exhibit precise site solution distributions.

*Electronic address: stanek@1an1.gov

[1] M. Tang, P. Lu, J. Valdez, and K. Sickafus, J. Appl. Phys. **99**, 063514 (2006).

[2] B. Antic, M. Mitric, and D. Rodic, J. Magn. Magn. Mater. **15**, 349 (1995).

[3] K. Wickersheim and R. Lefever, J. Electrochem. Soc. **111**, 47 (1964).

[4] A. Lempicki, C. Brecher, P. Szupryczynski, H. Lingertat, V. Nagarkar, S. Tipnis, and S. Miller, Nucl. Instrum. Methods Phys. Res. A **488**, 579 (2002).

[5] L. Pauling and M. Shappell, Z. Kristallogr. **75**, 128 (1930).

[6] B. O'Connor and T. Valentine, Acta Crystallogr., Sect. B: Struct. Crystallogr. Cryst. Chem. **B25**, 2140 (1969).

[7] E. Maslen, V. Streltsov, and N. Ishizawa, Acta Crystallogr., Sect. B: Struct. Sci. **B52**, 414 (1996).

[8] G. Blasse and B. Grabmaier, *Luminescent Materials* (Springer-Verlag, Berlin, 1994).

[9] E. Zych, J. Phys.: Condens. Matter **14**, 5637 (2002).

[10] H. Forest and G. Ban, J. Electrochem. Soc. **116**, 474 (1969).

[11] E. Zych, M. Karbowiak, K. Domagala, and S. Hubert, J. Alloys Compd. **341**, 381 (2002).

[12] M. Mandel, Appl. Phys. Lett. **2**, 197 (1963).

[13] M. Mitric, B. Antic, M. Balanda, D. Rodic, and M. L. Napijalo, J. Phys.: Condens. Matter **9**, 4103 (1997).

[14] D. Rodic, B. Antic, and M. Mitric, J. Magn. Magn. Mater. **140-144**, 1181 (1995).

[15] M. Mitric, P. Onnerrud, D. Rodic, R. Tellgren, A. Szytula, and M. L. Napijalo, J. Phys. Chem. Solids **54**, 967 (1993).

[16] H. Hintzen and H. van Noort, J. Phys. Chem. Solids **49**, 873 (1988).

[17] A. Grill and M. Schieber, Phys. Rev. B **1**, 2241 (1970).

[18] S. Kern and R. Kostelecky, J. Appl. Phys. **42**, 1773 (1971).

[19] B. Antic, M. Mitric, and D. Rodic, J. Phys.: Condens. Matter **9**, 365 (1997).

[20] G. Concas, G. Spano, M. Bettinelli, and A. Speghini, Z. Naturforsch., A: Phys. Sci. **58**, 551 (2003).

[21] G. Concas, G. Spano, E. Zych, and J. Trojan-Piegza, J. Phys.: Condens. Matter **17**, 2597 (2005).

[22] G. Concas, C. Muntoni, G. Spano, M. Bettinelli, and A. Speghini, Z. Naturforsch., A: Phys. Sci. **56**A, 267 (2001).

[23] E. Zych, D. Hreniak, and W. Strek, J. Alloys Compd. **341**, 385 (2002).

[24] M. Born, *Atomtheorie des Festen Zustandes* (Teubner, Leipzig, 1923).

[25] R. Buckingham, Proc. R. Soc. London, Ser. A **168**, 264 (1938).

[26] S. Vyas, R. Grimes, D. Gay, and A. Rohl, J. Chem. Soc., Faraday Trans. **94**, 427 (1998).

[27] M. Levy, R. Grimes, and K. Sickafus, Philos. Mag. **84**, 533 (2004).

[28] C. Stanek, M. Levy, K. McClellan, B. Uberuaga, and R. Grimes, Phys. Status Solidi B **242**, R113 (2005).

[29] C. Stanek, K. McClellan, M. Levy, and R. Grimes, J. Appl. Phys. **99**, 113518 (2006).

[30] C. Stanek, K. McClellan, M. Levy, and R. Grimes, Phys. Status Solidi B **243**, R75 (2006).

[31] B. Dick and A. Overhauser, Phys. Rev. **112**, 90 (1958).

[32] N. Mott and M. Littleton, Trans. Faraday Soc. **34**, 485 (1938).

[33] *Computer Simulation of Solids*, edited by C. Catlow and W. Mackrodt (Springer-Verlag, Berlin, 1982).

[34] R. Shannon, Acta Crystallogr., Sect. A: Cryst. Phys., Diffr., Theor. Gen. Crystallogr. **32**, 751 (1976).

[35] L. Petit, A. Svane, Z. Szotek, and W. M. Temmerman, Phys. Rev. B **72**, 205118 (2005).

[36] N. Hirosaki, S. Ogata, and C. Kocer, J. Alloys Compd. **351**, 31 (2003).

[37] F. Hanic, M. Hartmanová, G. Knab, A. Urusovskaya, and K. Bagdasarov, Acta Crystallogr., Sect. B: Struct. Sci. **40**, 76 (1984).

[38] Y. Malinovskii and O. Bondareva, Kristallografiya **38**, 1558 (1991).

[39] G. Kresse and J. Hafner, Phys. Rev. B **47**, 558 (1993).

[40] G. Kresse and J. Hafner, Phys. Rev. B **49**, 14251 (1994).

[41] G. Kresse and J. Furthmüller, Comput. Mater. Sci. **6**, 15 (1996).

[42] G. Kresse and J. Furthmüller, Phys. Rev. B **54**, 11169 (1996).

[43] P. E. Blöchl, Phys. Rev. B **50**, 17953 (1994).

[44] G. Kresse and D. Joubert, Phys. Rev. B **59**, 1758 (1999).

[45] H. Monkhorst and J. Pack, Phys. Rev. B **13**, 5188 (1976).

[46] M. Buijs, A. Meyerink, and G. Blasse, J. Lumin. **37**, 9 (1987).

[47] D. Klaasen, R. van Ham, and T. van Rijn, J. Lumin. **43**, 261 (1989).

[48] J. Heber and U. Köbler, in *Luminescence of Crystals, Molecules and Solutions*, edited by F. Williams (Plenum, New York, 1973), p. 379.

[49] R. Pappalardo and R. Hunt, J. Electrochem. Soc. **132**, 721 (1985).

[50] T. Förster, Ann. Phys. **2**, 55 (1948).

[51] D. Dexter, J. Chem. Phys. **21**, 836 (1953).

[52] H. Dornauf and J. Heber, J. Lumin. **22**, 1 (1970).